ISSN: 2319-5967
ISO 9001:2008 Certified
International Journal of Engineering Science and Innovative Technology (IJESIT)
Volume 6, Issue 1, January 2017

Spectroscopic Analysis of Zinc doped Cobalt Ferrite nanoparticles

Sheena Xavier, Vimala George, Aleena Jose, Karthi Krishna M.R, Jonis V.C.

Abstract* — Spinel ferrites are the most interesting magnetic oxides due to their interesting magnetic, electrical and optical properties. Zinc doped cobalt ferrite spinel nanoparticles were prepared by the sol gel synthesis. All the samples were characterized by using X-ray diffraction technique (XRD), TEM, UV–visible diffuse reflectance spectroscopy and Fourier transformed infrared (FTIR) spectroscopy. The XRD patterns confirmed the formation of single phase inverse spinel structure without impurities. The lattice parameter increased from 8.315 to 8.354 Å with increasing Zn^{2+} concentration. The average crystallite size obtained by Scherrer method varies between 17.191 nm and 13.699 nm. The oxygen parameter decreases with increase in zinc ion concentration. The X-ray densities for different samples were estimated and are in good agreement with the reported value. The band gap energy values obtained from UV- visible analysis, increases with an increase in zinc ion concentration (2.276 –2.325 eV). FTIR spectrum analysis were carried out and the absorption spectra shows two significant absorption bands between 350 cm^{-1} and 4000 cm^{-1}, which is attributed to tetrahedral (A) and octahedral (B) sites of the spinel phase. The results obtained in the present study suggests that the $Co_{1-x}Zn_xFe_2O_4$ (x=0.0 to 0.5) nanostructures prepared by sol-gel synthesis can be useful in optoelectronic applications.

Index Terms — **Band gap, cobalt ferrite, ferrites, spinels.**

I. INTRODUCTION

Recently, oxides of iron have created particular interest in different areas of science and technology [1]. Because of their characteristic magnetic, electrical and optical properties, spinel ferrites are the widely studied and the mostly used magnetic oxides. As they possess excellent properties like high electrical resistivity and high permeability, they are best for the manufacturing microwave devices, telecommunication equipments, high density magnetic storage, magnetic fluids, gas sensors etc. [2].

The spinel structure has the general formula AB_2O_4, in which A represents a divalent metal ion and B represents a trivalent metal ion. Spinel structure can be described as a cubic close-packed arrangement of oxygen atoms with eight formula units per unit cell. In the unit cell, there are 64 tetrahedral sites and 32 octahedral sites out of which only 8 tetrahedral sites and 16 octahedral sites are respectively occupied by the A and B atoms. In A site the divalent metal ion is in the center of a tetrahedron surrounded by four oxygen atoms, whereas in B site, the trivalent metal ion is in the center of an octahedron and is surrounded by six oxygen atoms. In general, spinels are classified into three types; viz, normal, inverse and mixed. The normal spinel can be represented by $[A]_{tet}[B]_{oct}O_4$ whereas the inverse spinel by $[B]_{tet}[A,B]_{oct}O_4$ [3].

The properties of ferrites are influenced by their composition. Cobalt ferrite is an important one among the various ferrites because of its unique properties. Further, the substitution of a diamagnetic ion like Zn brings about interesting changes in the properties of cobalt ferrite. This is because Zn ions seek to the tetrahedral sites of the ferrite sub-lattice, resulting in a decreased magnetic moment [4].

Nano sized particles of ferrite class of compounds exhibit enhanced properties compared to their bulk counterparts [5]-[7]. The properties of nanoferrites strongly depend on the particle size too [8-10]. Reports supporting the relation between surface structure and magnetic properties are available [11]-[12]. Various methods for synthesizing ferrite nanoparticles have been reported in literature. The different methods include solid state reaction [13], combustion synthesis [14], the electrochemical method [15], micro-emulsions [16], the sol –gel process [17], ball milling [18], microwave processing [19] etc.

In the present work we report the synthesis of various concentrations of Zn doped Co ferrite by the sol – gel method. The structural details of the prepared samples were studied using XRD patterns. Furthermore, the improvement of optical properties of Co ferrite with increasing Zn content is also studied by analyzing the UV-Vis and FTIR spectra of different samples.

ISSN: 2319-5967
ISO 9001:2008 Certified
International Journal of Engineering Science and Innovative Technology (IJESIT)
Volume 6, Issue 1, January 2017

II. EXPERIMENTAL METHOD

A. Sample Preparation

Nano particles of zinc doped cobalt ferrites were synthesized by the sol-gel method. Appropriate weights of cobalt nitrate, zinc nitrate and ferric nitrate were dissolved in minimum amount of ethylene glycol using a magnetic stirrer at about 40°C. The solution of the metal compounds was heated at 60°C and a wet gel was obtained. The obtained gel was dried by increasing the temperature and finally self-ignites to give a product which is fluffy and highly voluminous. A redox reaction takes place here, with the nitrate ion as the oxidant and the ethylene glycol as the reducing agent. The organic component gets decomposed by the nitrate ion by setting an oxidising environment. The obtained powder was ground well using agate mortar and sintered at 500°C for four hours.

B. Characterisation Techniques

The structural characterization of zinc doped cobalt ferrite series was done by recording the X-ray diffraction (XRD) of the samples. The X-ray diffraction patterns were recorded using Bruker AXS D8 Advanced X-ray diffractometer with Cu-Kα (λ=1.5406A^0) radiation at 30KV and 20mA. The lattice parameter '*a*' was then computed by assuming cubic symmetry using equation

$$d_{hkl} = \frac{a}{\sqrt{h^2+k^2+l^2}} \qquad (1)$$

where d_{hkl} is the lattice spacing of planes with miller indices (hkl).
The diffraction peaks are broad indicating the nanometer size of the crystallite. The particle size of the samples has been estimated from the broadening of XRD peaks using the Scherrer equation given by

$$t = \frac{0.9\lambda}{\beta Cos\theta_B} \qquad (2)$$

with β as the FWHM and θ_B as the angle of diffraction.

In Ferrites, the formation of fcc structure by the oxygen ions is true only to a certain extent. In reality, slight deviations are found owing to a deformation caused by the metal ions. Also, the tetrahedral sites, which are smaller than octahedral ones, are too small to contain a metal ion, if the metal ions as well as the oxygen ions are regarded as solid spheres. As a consequence, all the tetrahedral sites are expanded by an equal displacement of the four oxygen ions outwards along the body diagonals of the cube. These four oxygen ions still occupy the corners of an enlarged tetrahedron, in such a way that it retains the cubic symmetry. A quantitative measure of this displacement is the oxygen parameter u which is calculated as follows.

A simple calculation shows that for small displacements the radii of the spheres in both the types of interstitial sites are given by,

$$r_A = \left(u - \frac{1}{4}\right) a\sqrt{3} - R_0 \qquad (3)$$

$$r_B = \left(\frac{5}{8} - u\right) a - R_0 \qquad (4)$$

where R_0 is the radius of oxygen ion, u is the oxygen parameter.

By solving (3) and (4)

$$u = \frac{(r_A - r_B) + a(1.058)}{a(\sqrt{3}+1)} \qquad (5)$$

The diffuse reflectance spectrum in the UV – visible range was recorded using Shimadzu UV-2600 spectrophotometer to estimate the variation of optical band gap with increasing Zn content. Using UV-Visible analysis, the optical band gap (E_g) is given by the equation,

$$\alpha E_p = A(E_p - E_g)^q \qquad (6)$$

ISSN: 2319-5967
ISO 9001:2008 Certified
International Journal of Engineering Science and Innovative Technology (IJESIT)
Volume 6, Issue 1, January 2017

where α is the absorption coefficient, E_p is the photon energy, A is a constant and q depends on the nature of transition. The above equation is solved for direct and indirect band gap semiconductors as follows:
For indirect band gap,

$$\alpha h\upsilon = A(h\upsilon - E_g)^2 \qquad (7)$$
$$(\alpha h\upsilon)^{\frac{1}{2}} = A^{1/2}(h\upsilon - E_g)$$

For direct band gap,

$$\alpha h\upsilon = A(h\upsilon - E_g)^{1/2} \qquad (8)$$
$$(\alpha h\upsilon)^2 = A(h\upsilon - E_g)$$

The values of the band gaps were estimated by the intercepts made on the X-axis by extrapolated linear portion of the graphs.

IR spectra of the investigated nano ferrite samples were recorded using FTIR spectrometer (spectrum two, PerkinElmer) in the wave number range 4000 to 350 cm^{-1}.

III. RESULTS AND DISCUSSION

A. XRD Analysis

The observed XRD pattern of the samples matches well with the reported patterns [19] confirming the spinel type structure of the samples. The crystal structure and phase purity of pure and zinc doped cobalt ferrite samples were confirmed from the X-ray diffraction pattern shown in Fig.1. The diffraction peaks at 2θ values 30.407, 35.66, 43.426, 53.750, 57.241 and 62.826 are indexed to (220), (311), (400), (511) and (440) reflection planes of cobalt ferrite respectively. All the peaks match well with the JCPDS card No. 22-1086 signifying the cubic spinel formation. There are no additional peaks attributing to the impurity phases.
As given in Table I, estimated crystallite size for pure and zinc doped cobalt ferrites decreases with increase in Zn^{2+} ion concentration due to the lower bond energy of Zn^{2+}- O^{2-}as compared to Co^{2+}-O^{2-}. It is inferred that the lattice parameter 'a' of $CoFe_2O_4$ is in good agreement with the reported value (8.383 A^o) [20]. As the zinc ion concentration increases, lattice parameter also increases. This increase in lattice parameter with increase in Zn^{2+} concentration indicates the occurrence of lattice expansion without disturbing the lattice symmetry. This is due to the fact that the size of Zn^{2+} ion radius (0.74 A^o) is larger than the radius of Co^{2+} ion radius (0.70 A^o). The values of oxygen parameter (u) are obtained from the radii of the tetrahedral site r_A and octahedral site r_B and plotted as a function of zinc content, x as shown in the Fig.2.

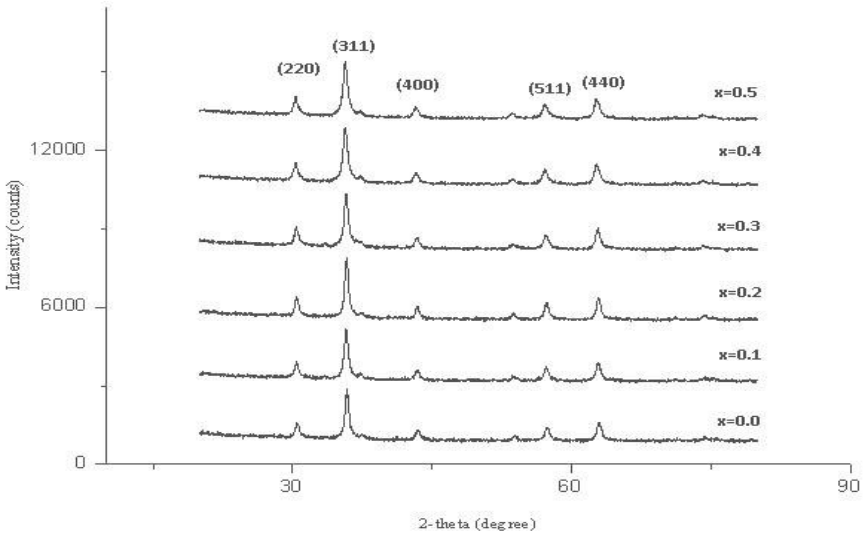

Fig. 1 XRD patterns of $Co_{1-x}Zn_xFe_2O_4$

ISSN: 2319-5967
ISO 9001:2008 Certified
International Journal of Engineering Science and Innovative Technology (IJESIT)
Volume 6, Issue 1, January 2017

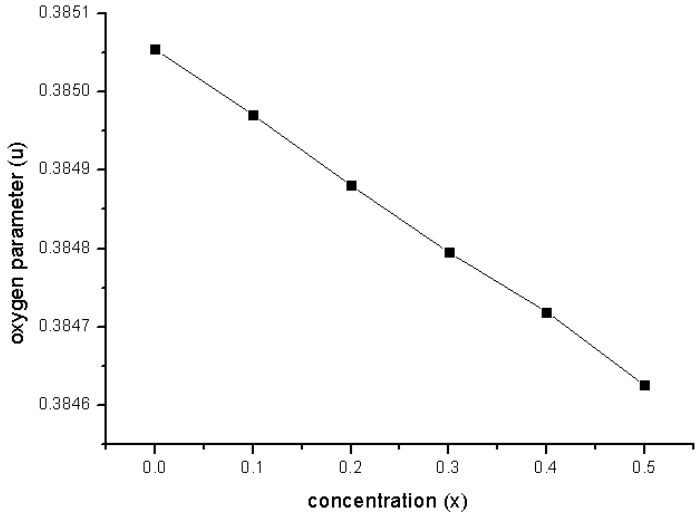

Fig.2 The oxygen parameter as a function of concentration

Due to the reasons mentioned earlier, u is found to decrease with the increase in Zn content. The X-ray density for different samples is estimated and tabulated. They are in good agreement with theoretically reported values.

Table I Compositional dependence of the structural parameters

Sample	Lattice parameter(a) (A^0)	Particle size t (nm)	Density d (g/cm^3)	Oxygen parameter (u)
CZ0	8.315	17.191	5.425	0.38505
CZ1	8.332	16.717	5.405	0.38497
CZ2	8.325	17.928	5.434	0.38488
CZ3	8.334	16.638	5.430	0.38479
CZ4	8.354	15.443	5.407	0.38472
CZ5	8.354	13.699	5.421	0.38463

B. TEM

The particle size distribution of the nanoparticles as observed in TEM images is shown in Fig. 3. It can be seen that the samples have narrow size distribution. The image reveals that most of the nanoparticles are almost spherical in shape.

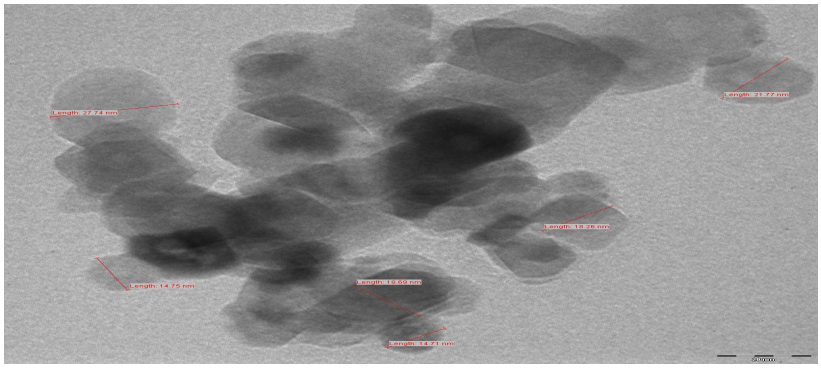

Fig 3.TEM image of $Co_{0.8}Zn_{0.2}Fe_2O_4$

ISSN: 2319-5967
ISO 9001:2008 Certified
International Journal of Engineering Science and Innovative Technology (IJESIT)
Volume 6, Issue 1, January 2017

C. UV Analysis

The diffuse reflectance spectra (DRS) are a standard tool to determine the optical band gap of the nanoparticles. The band gap values of cobalt ferrites were calculated using the Tauc relation. The plots of $h\nu$ versus $(\alpha h\nu)^2$ for all the samples are shown in Fig.4. Extrapolation of linear regions of these plots gives the direct band gap values. The estimated bandgap values of $Co_{1-x}Zn_xFe_2O_4$ with x = 0.1, 0.2, 0.3, 0.4, and 0.5 are given in Table II. By analysing the table it is clear that, on doping with the Zn ions the bandgap goes on increasing with increase in Zn concentration in cobalt ferrite which is attributed to the quantum confinement phenomenon. The decrease in crystal size with increasing the optical bandgap confirms the quantum size effect.

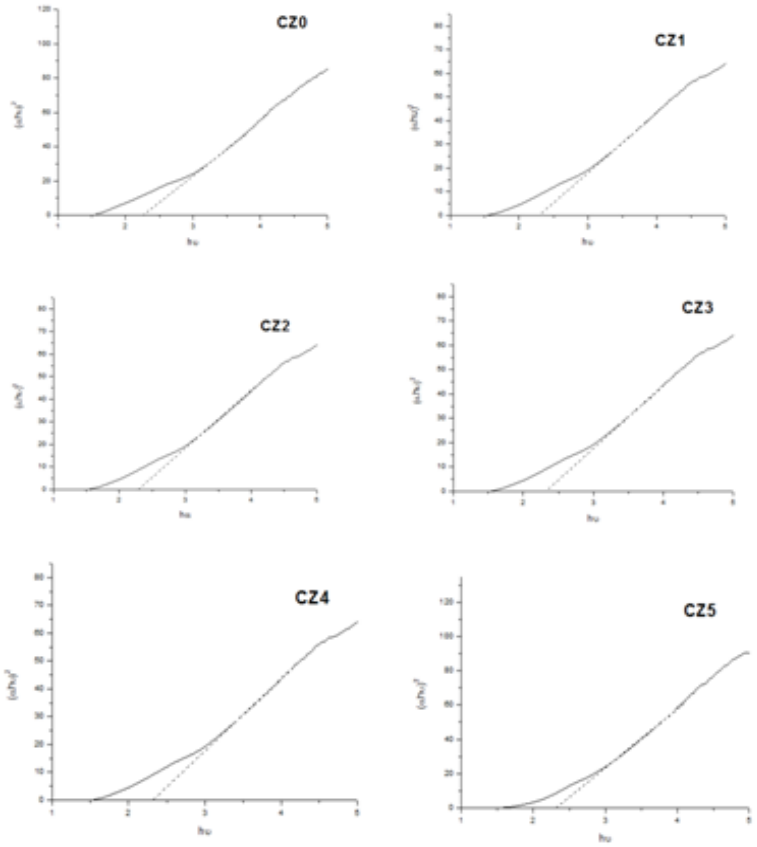

Fig.4 UV-Vis spectra of $Co_{1-x}Zn_xFe_2O_4$ nanoparticles

Table II Band gap energy of $Co_{1-x}Zn_xFe_2O_4$

Sample	Band gap energy, E_g (eV)
CZ0	2.276
CZ1	2.287
CZ2	2.292
CZ3	2.303
CZ4	2.313
CZ5	2.325

D. FTIR Analysis

FTIR spectra of $Co_{1-x}Zn_xFe_2O_4$ samples in the wavenumber range 1000-350 cm^{-1} are shown in Fig.5 and the vibrational frequencies of the IR bands are given in Table III. The absorption bands observed in the range 600-550 cm^{-1} and 400-350cm^{-1} are characteristics of the spinel ferrites and no peaks were observed in the range 4000-1000

ISSN: 2319-5967
ISO 9001:2008 Certified
International Journal of Engineering Science and Innovative Technology (IJESIT)
Volume 6, Issue 1, January 2017

cm^{-1}. The higher frequency band (ν_1) corresponds to intrinsic vibrations of the metal-oxygen bond at the tetrahedral site and the lower frequency band (ν_2) is caused by metal oxygen vibration in the octahedral site. These absorption bands depends on metal-oxygen bond strength and bond length which in turn changed by the substitution of zinc for cobalt ion. The bands arise from the lattice vibrations of oxide ions against the cations. The frequency band found at about 559.78cm^{-1} is due to the intrinsic stretching vibrations of the tetrahedral sites of Fe^{3+}- O^{2-}. The band at 404.41 cm^{-1} is attributed to the octahedral group of Co^{2+} - O^{2-}. It is found that Fe-O distance of A sites (1.89 A^o) is smaller than that of B site (1.99A^o). This can be interpreted by the more covalent bonding of Fe^{3+} ions at the A sites than B sites. Therefore the tetrahedral stretching mode is observed at higher wave number than octahedral due to shorter bond length of Fe-O in tetrahedral symmetry. These two absorption bands observed within this limit reveal the formation of single phase spinel structure having two sub-lattices, tetrahedral site (A) and octahedral site (B). The vibration band ν_1 shows a constancy with the increase in Zn^{2+} ion content and absorption band ν_2 is shifted towards higher frequency with value varying from 404.41 - 379.39cm^{-1} with the addition of Zn^{2+}ions. This shifting of absorption band ν_2 towards higher frequency which in turn increase the bond length at B-site suggests that the substituted metal ion occupies the B-site.

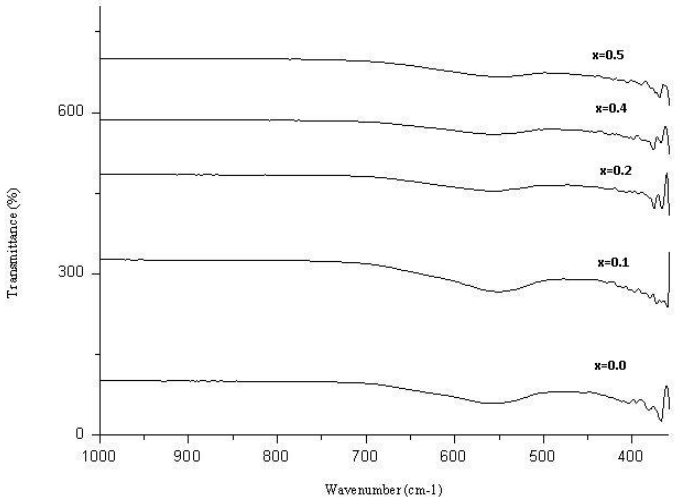

Fig.5 FTIR spectra of $Co_{1-x}Zn_xFe_2O_4$

Table III Absorption bands of $Co_{1-x}Zn_xFe_2O_4$

Sample	Absorption band, ν_1(cm^{-1})	Absorption band, ν_2 (cm^{-1})
CZ0	559.66	404.41
CZ1	549.16	390.41
CZ2	559.78	390.00
CZ4	559.78	379.39
CZ5	559.78	379.39

IV. CONCLUSION

Nanostructured pure and zinc substituted cobalt ferrite was successfully prepared by the sol-gel synthesis. The XRD pattern matched well with the JCPDS card number 22-1086 signifying the cubic spinel structure. The analysis of XRD data revealed that increase in Zinc content decreases the crystalline size of the samples. The lattice parameter increased with increasing zinc concentration, due to the substitution of Zn in the cobalt sites. UV absorption study on sample shows that band gap energy increases with Zn concentration. Quantum confinement phenomena were observed with increasing the zinc content in the doped cobalt ferrite system. FTIR spectra showed the band at about 559 cm^{-1} is due to the intrinsic stretching vibrations of the tetrahedral sites of Fe^{3+}- O^{2-} . The band at 382cm^{-1} and 296 cm^{-1} is attributed to the octahedral group of Co^{2+} - O^{2-}. The results obtained in the present study suggests that the $Co_{1-x}Zn_xFe_2O_4$ (x=0.0 to 0.5) nanostructures pre-pared by sol-gel synthesis can be a potential candidate in optoelectronic applications.

ISSN: 2319-5967
ISO 9001:2008 Certified
International Journal of Engineering Science and Innovative Technology (IJESIT)
Volume 6, Issue 1, January 2017

As the bandgap of the samples increases with increasing the Zn doping, this has a scope in solar cell applications also, which is to be tested in the future works.

ACKNOWLEDGMENT

We acknowledge the financial support of DST through FIST project. We also thank Ms. Fousymol T.M. for the fruitful suggestions and support given during this work.

REFERENCES

[1] Ulises A.Agu, Marcos I. Olivia, Sergio G.Marchetti, Angelica C Heredia, Sandra G.Casuscelli, Monica E. Crivello "Synthesis and Characterisation of a mixture of CoFe2O4 and MgFe2O4 from layered double hydroxides: Band gap energy and magnetic responses", journal of magnetism and magnetic materials 369, pp249-259, 2014.

[2] Seem Joshi, Manoj Kumar, Sandeep Chokkar, Geetika Srivastava, Mukesh Jewariya,V.N.Singh" Structural, magnetic, dielectric and optical properties of nickel ferrite nanoparticles synthesized by co-precipitation method", J. of Molecular Structure, vol.1076, pp. 55-62 ,2014.

[3] A. Goldman, Modern Ferrite Technology, Van Nostrand, New York, 1990.

[4] C. Singh, S. Jauhar, V. Kumar, J. Singh, S. Singhal, "Synthesis of zinc substituted cobalt ferrites via reverse micelle technique involving in situ template formation: A study on their structural, magnetic, optical and catalytic properties", Materials Chem. and Phys., vol. 156, pp. 188-197, 2015.

[5] K Nivethitha Lakshmi and Dr.J. Santhananalakshmi, "Synthesis, Size Characterisation and Photocatalytic Activities of Zinc Ferrites and Cobalt Ferrites Nanoparticles using Oxidative Degradations of Methylene Blue, Crystal Violet and Alizarin Red Dyes in Aqueous Medium at 25^{o}C",Int.J. of Innovative Research in Sci. & Eng. ISSN (online) 2347- 3207.

[6] N. Gupta, A. Verna, S.C.Kashyapa and D.C. Dube, "Microstructural, dielectric and magnetic behavior of spin-deposited nanocrystalline nickel–zinc ferrite thin films for microwave applications", J. Magn. Magn. Mater. Vol.308, pp.137-142, 2007.

[7] M.Srivastava, Animesh K.Ojh, S.Chaubey, and A.Matemay, "Synthesis and Optical characterization of nanocrystalineNiFe_2O_4 structures", J.alloys compnds, vol. 481,pp.515-519,29 July 2009.

[8] Sujoy Roy, Igor Dubenko, Dossah D. Edorh, and naushad Ali "Size induced variations in structural and magnetic properties of double exchange $La_{0.8}Sr_{0.2}MnO_{3-\delta}$ nano ferromagnet", vol. 96, pp. 1202-1208, June 2004.

[9] M.E. McHenry, D.E.Laughlin, "Nano-scale materials development for future magnetic applications", vol. 48, pp. 223-238, 1 January 2000.

[10] John Jacob, M.Abdul Khadar, "VSM and Mossbauer study of nanostructured hematite", J. Magn. Magn. Mater, Vol. 322, pp. 614-621, March 2010.

[11] S. Son, R. Swaminathan, and M.E. McHenry "Structure and magnetic properties of rf thermally plasma synthesised Mn and Mn-Zn ferrite nanoparticles" J. Appl. phys, vol.93, pp. 7495-7497, May 2003.

[12] R. Swaminathan, M.E. McHenry, P.Poddar, H.Srikanth, "Magnetic properties of polydisperse and monodisperse NiZn ferrite nanoparticle interpreted in a surface structure model" , J. Appl. Phys.97(10), pp.1-3,2005.

[13] Z. Sun, L. Liu, D. Jia, W.pen, "simple synthesis of $CuFe_2O_4$ nanoparticles as gas sensing materials", Sensors and Actuators B, Vol.125 (1), pp.144-148, 2007.

[14] E. Ranjith Kumar, R.Jayaprakash, G. Sarala Devi, P.Siva Prasada Reddy " Magnetic, dielectric and sensing properties of manganese substituted copper ferrite nanoparticles" , J. Magnet. magnet. Mater, vol. 355, pp- 87-92, April 2014.

[15] P. Pulisova, J. Kovac, A. Voigt, P. Raschman "Structure and magnetic properties of Co and Ni nano-ferrites prepared by a two step direct microemulsions synthesis", J. Magnet. magnetometer, vol.341, pp.93–99 (2013).

[16] A.V. Raut, R.S. Barkuule, D.R. Shengule, K..M. Jadhav, "Synthesis, structural investigation and magnetic properties of Zn^{2+} substituted cobalt ferrite nanoparticles prepared by the sol–gel auto-combustion technique", J.Magn.Magn.Mater, vol.358–359, pp.87–92 , May 2014.

[17] M.E. Arani, M.J. Javad Isfahani, M.A. Kashi, "Preparation and magnetic studies of nickel ferrite nanoparticles substituted by$Sn^{4+}$and Cu^{2+}", J.Magnet.Magnet.Mater, Vol.322, pp.2944–2947, October 2010.

[18] Karcioglu Karakas, Zeynep, Boncukcuglu, Recep, Karakas, Ibrahim Hakki, Ert ugrul, Mehmet, "The effects of heat treatment on the synthesis of nickel ferrite ($NiFe_2O_4$) nanoparticles using the microwave assisted combustion method", J.Magn.Magn.Mater, vol.374, pp. 298–306, 2015.

ISSN: 2319-5967
ISO 9001:2008 Certified
International Journal of Engineering Science and Innovative Technology (IJESIT)
Volume 6, Issue 1, January 2017

[19] M Sundararajan, L John Kennedy, Udaya Aruldoss, Sk.Khadeer Pasha, Judith Vijaya, Steve Dunn "Microwave combustion synthesis of zinc substituted nanocrystalline spinel cobalt ferrite: Structural and magnetic studies" Mat Sci. in Semiconductor processing vol.40, pp.1-10, 2015.

[20] Ya Tang, Xinwei Wang, Qinghong Zhang, Hongzhi Wang, "Solvothermal synthesis of $Co_{1-x}Ni_xFe_2O_4$ nanoparticles and its application in ammonia vapour detection", Prog. Nat. Sci: Mater. In. Vol 22, pp.53 -58, February 2012.

AUTHOR BIOGRAPHY

Dr. Sheena Xavier, Associate Professor in Physics, St. Xavier's College for Women, Aluva, Kerala, India is the Reviewer of two international Journals. She has 26 publications in various International/ National Journals/ Conference Proceedings.

Dr. Vimala George, Assistant Professor in Physics, St. Xavier's College for Women, Aluva has 5 published papers in International Journals/ Proceedings.

Ms. Aleena Jose is doing her post graduation in Dept. of Physcis, St. xavier's College for Women, Aluva